RAT BRAIN GLUCOSE TRANSPORTER-2, INSULIN RECEPTOR AND GLIAL EXPRESSION ARE ACUTE TARGETS OF INTRACEREBROVENTRICULAR STREPTOZOTOCIN: RISK FACTORS FOR SPORADIC ALZHEIMER'S DISEASE?

Knezovic A[1], Loncar A[1,2], Homolak J[1], Smailovic U[1,3], Osmanovic Barilar J[1], Ganoci L[4], Bozina N[1,4], Riederer P[5], Salkovic-Petrisic M[1*]

[1] Department of Pharmacology and Croatian Institute for Brain Research, University of Zagreb School of Medicine, Zagreb, Croatia

[2] Department of Neurology, General Hospital Karlovac, Karlovac, Croatia

[3] Department of Neurobiology, Care Sciences and Society, Division of Clinical Geriatrics, Karolinska Institute, Stockholm, Sweden

[4] Department of Laboratory Diagnostics, University Hospital Centre Zagreb, Zagreb, Croatia

[5] Centre of Mental Health, Department of Psychiatry, Psychosomatics, and Psychotherapy, University Hospital of Würzburg, Würzburg, Germany

*Corresponding author: Melita Salkovic-Petrisic
e-mail address: melitas@mef.hr
Phone number: +38514590219
Postal address: Department of Pharmacology
University of Zagreb School of Medicine
Salata 11
10 000 Zagreb
Croatia

ABSTRACT

Accumulated evidence suggests that the insulin resistant brain state and cerebral glucose hypometabolism might be the cause, rather than the consequence, of the neurodegeneration found in a sporadic Alzheimer's Disease (sAD). We have explored whether the insulin receptor (IR) and the glucose transporter-2 (GLUT2), used here as their markers, are the early targets of intracerebroventricularly (icv) administered streptozotocin (STZ) in a STZ-icv rat model of sAD, and whether their changes are associated with the STZ-induced neuroinflammation. The expression of IR, GLUT2 and glial fibrillary acidic protein (GFAP) was measured by immunofluorescence and Western blot analysis in the parietal (PC) and the temporal (TC) cortex, in the hippocampus (HPC) and the hypothalamus (HPT). One hour after the STZ-icv administration (1.5 mg/kg), the GFAP immunoreactivity was significantly increased in all four regions, thus indicating the wide spread neuroinflammation, pronounced in the PC and the HPC. Changes in the GLUT2 (increment) and the IR (decrement) expression were mild in the areas close to the site of the STZ injection/release but pronounced in the ependymal lining cells of the 3rd ventricle, thus indicating the possible metabolic implications. These results, together with the finding of the GLUT2-IR co-expression, and also the neuronal IR expression in PC, TC and HPC, indicate that the cerebral GLUT2 and IR should be further explored as the possible sAD etiopathogenic factors. It should be further clarified whether their alterations are the effect of a direct STZ-icv toxicity or they are triggered in a response to STZ-icv induced neuroinflammation.

Keywords: streptozotocin, Alzheimer's disease, glucose transporter 2, insulin receptor

INTRODUCTION

Alzheimer's disease (AD) is the most common type of dementia in the world today, however the precise etiology and pathogenesis of the predominanting sporadic form (sAD), still remain to be clarified. Recently accumulated evidence support the concept that the insulin resistant brain state (IRBS) and the cerebral glucose hypometabolism might be the pathological core of sAD (Chen and Zhong 2013; De Felice et al. 2014; Chen et al. 2014a; de la Monte and Tong 2014). IRBS is a condition molecularly characterized by the reduced response to insulin signaling downstream the insulin receptor (IR) - phosphatidylinositol -3 kinase (PI-3K) pathway in the brain. Considering the neurotrophic, neuroprotective and neuromodulatory role of brain insulin, IRBS leads to the neurodegeneration and cognitive impairment in an animal model of sAD (Lester-Coll et al. 2006; Agrawal et al. 2011; Barilar et al. 2015; Knezovic et al. 2015). IRBS was also found in sAD patients post-mortem (Frölich et al. 1998; Steen et al. 2005; Talbot et al. 2012; Yarchoan et al. 2014; Stanley et al. 2016). It represents a brain-related metabolic syndrome, associated with the metabolic and oxidative stress and the neuroinflammation of the brain, which may or may not be accompanied by the alterations in the peripheral metabolic homeostasis, since diabetes type 2 (T2DM) increases the risk for AD (and vice versa). However, not all T2DM patients develop AD (and vice versa) and the AD is not necessarily associated with hyperglycemia (Blázquez et al. 2014; Talbot 2014).

While IRBS can be detected only post-mortem, giving no clue on the time of its onset, the neuroimaging technology has enabled *in vivo* visualization of the impairment in the cerebral glucose metabolism of sAD patients (2-[18F]fluoro-2-deoxy-d-glucose PET /FDG-PET/ studies. This impairment was found especially in the parietotemporal and the frontal association cortices, and was pronounced in hippocampus, which has high glucose demands and insulin sensitivity (Mosconi 2005). Although still not well understood, the impairment of cerebral glucose uptake/metabolism in sAD appears to be the cause, rather than the consequence of neurodegeneration found in sAD, as it appears to precede cognitive dysfunction for many years. Two-year follow-up study of the cognitively normal individuals (aged 50-82 years) demonstrated that the maternal history of AD predisposed them to the baseline reductions in the brain glucose metabolism of the AD-vulnerable brain regions, which significantly

progressed over the follow-up time, in comparison to those with maternal AD negative or paternal AD positive history (Mosconi et al. 2009). Furthermore, late middle aged cognitively normal subjects (50-65 years), who were homozygous for the *e*4 allele for apolipoprotein E and reported a family history of probable AD, had reduced glucose metabolism on PET images in the same regions of the brain as the patients with probable AD (Reiman et al. 1996). Although these findings do not directly prove the cerebral hypometabolism as the earliest event in AD, they are currently the earliest known measurable abnormality in the brain connected to AD (Cunnane et al. 2011).

Specific nature of AD and a long presymptomatic phase do not allow the exploration of the precise onset of IRBS and the cerebral glucose hypometabolism as the possible etiopathogenic factors during the life-time of sAD patients, which is why the animal models of sAD are used to enlighten this problem.

The non-transgenic rat model that has been proposed as a model of sAD is generated by intracerebroventricular administration of low-dosed streptozotocin (2-deoxy-2-(3-methyl-3-nitrosoureido)-D-glucopyranose; so called STZ-icv model (Hoyer 1998; Lannert and Hoyer 1998). Indeed, STZ-icv application to rats induces progressive deficits in learning and memory (Mayer et al. 1990; Saxena et al. 2008; Knezovic et al. 2015) and neurochemical and neuropathological alterations in the brain that resemble those found in sAD patients (Salkovic-Petrisic and Hoyer 2007); decreased cholinergic transmission (Blokland and Jolles 1993; Agrawal et al. 2009; Biasibetti et al. 2017), oxidative stress (Sharma and Gupta 2001; Dias et al. 2014; Prakash et al. 2015) and neuroinflammation (Prickaerts et al. 1999; Kraska et al. 2012; Biasibetti et al. 2017), tau hyperphosphorylation and early neurofibrillary changes (Deng et al. 2009; Barilar et al. 2015; Knezovic et al. 2015), and pathological accumulation of amyloid β 1-42 (Aβ1-42) in meningeal and cortical capillaries (Salkovic-Petrisic et al. 2006; Salkovic-Petrisic et al. 2011), neurons and eventually in primitive plaque-like formations (Knezovic et al. 2015). Most importantly, in addition to all these pathologies, the STZ-icv rat model generates IRBS (Lester-Coll et al. 2006; Grünblatt et al. 2007; Agrawal et al. 2011; Barilar et al. 2015) and demonstrates reduction in cerebral glucose/energy metabolism (Plaschke and Hoyer 1993; Hoyer et al. 1994; Hoyer and Lannert 2007). IRBS induced by STZ-icv

administration is characterized by the decrease in insulin receptor (IR) mRNA and protein expression and the IR signalling dysfunction downstream of the PI-3K pathway in particular brain regions, resulting in the increased activity of glycogen synthase kinase (GSK-3β) and the hyperphosphorylation of tau protein (Lester-Coll et al. 2006; Agrawal et al. 2011; Barilar et al. 2015). Reduction in cerebral glucose metabolism in the STZ-icv rat model has been found in 17 of 35 rat brain areas, particularly in the frontal, parietal, sensory motor, auditory and entorhinal cortex and in all hippocampal subfields (Duelli et al. 1994), while significant decreases in the activities of glycolytic key enzymes were found in the brain cortex and hippocampus (Plaschke and Hoyer 1993).

STZ-icv mice model that shares the similar pathophysiology with STZ-icv rat model (cognitive deficits, IRBS, oxidative stress and neuroinflammation) has lately been introduced in a basic AD research (Chen et al. 2013; Li et al. 2016; Amiri et al. 2016). STZ-icv treatment of transgenic AD mice has been shown to exacerbate cognitive deficits as well as tau hyperphosphorylation and amyloid plaque formation (Plaschke et al. 2010) in addition to neuroinflammation (Chen et al. 2014b).

There are three important facts, which indicate why more attention should be paid to the STZ-icv-induced generation of IRBS and the development of cerebral glucose hypometabolism, considered to be the possible sAD etiopathogenic markers. Firstly, the peripheral administration of STZ induces diabetes mellitus type I (T1DM) after a single high dose of this compound, or insulin resistance and diabetes mellitus type 2 (T2DM) after its multiple low doses (Blondel and Portha 1989; Szkudelski 2001). It has been suggested that the diminished IR autophosphorylation and the kinase activity could provide a possible mechanism for the post-binding insulin resistance in diabetic rats, although it was not clear whether the diabetic metabolism rather than a toxic effect of STZ itself should account for this phenomenon (Kadowaki et al. 1984; Giorgino et al. 1992). Changes in IR autophosphorylation and tyrosine kinase activity have been found also in the brain of the STZ-icv rat model (Grünblatt et al. 2007), however it has been argued that the IR damage is caused directly by the icv injections of STZ (Grieb 2016). Secondly, STZ enters the cell as a selective substrate for the glucose transporter 2 (GLUT2), which is highly concentrated at the membrane of pancreatic β cells (Szkudelski 2001) but to a lesser extent is present also in the

brain (Brant et al. 1993; Arluison et al. 2004a; Arluison et al. 2004b). Not only has STZ been a selective substrate for the GLUT2 (and not for the other GLUTs), but i*n vitro* and *in vivo* studies have also demonstrated that GLUT2 itself is a key target molecule for STZ, which reduces GLUT2 protein expression and mRNA in a concentration-dependent manner (Wang and Gleichmann 1995; Wang and Gleichmann 1998; Gai et al. 2004). GLUT2 in the brain is involved in the glucose sensing and transportation, and the glucose transportation and intracellular oxidative catabolism are the two main processes which regulate cerebral glucose metabolism (Maekawa et al. 2000; Chen and Zhong 2013). Decreased intracellular oxidative catabolism of glucose has been demonstrated in the brain of STZ-icv rats (Plaschke and Hoyer 1993; Hoyer et al. 1994), but data on the alterations of the cerebral GLUT2 levels in this model are still lacking. Thirdly, the mechanism(s) of intracellular STZ toxicity in the pancreatic β cells is well known, and, together with the DNA damage, the decrement in the ATP level and the inhibition of *O*-GlcNAc-selective *N*-acetyl-*β*-D-glucosaminidase (O-GlcNAcase), it involves also the induction of nitrosative/oxidative stress with the generation of nitric oxide (NO), free radicals and hydrogen peroxide (Szkudelski 2001; Konrad et al. 2001). However, the mechanism of STZ toxicity is far less clear in the brain. Oxidative stress and neuroinflammation, as well as the mitochondrial abnormalities, are quite prominent pathological alterations in the brain of both, AD patients and STZ-icv rats (Prickaerts et al. 1999; Sharma and Gupta 2001; Kraska et al. 2012; Correia et al. 2013) however, it is not clear whether they precede IRBS and cerebral glucose metabolism dysfunction.

We have investigated whether IR and GLUT2 in the rat brain are the early targets of STZ following its icv administration, and if their changes are associated with the neuroinflammation. Our research was primarily focused on the brain regions involved in the cognition, i.e. parietotemporal cortex and hippocampus, but after the unexpected findings of the intensive immunoreactive neuroinflammatory signal in the hypothalamic region of the STZ-icv group, the histology analysis of the hypothalamus was also performed.

MATERIAL AND METHODS

Materials

STZ, protease inhibitor cocktail, paraformaldehyde, monoclonal mouse anti-β-actin and monoclonal mouse anti-GFAP antibodies, fluoroshield, and normal goat serum were purchased from Sigma-Aldrich (St. Louis, Missouri, USA). The anti-GLUT2 (rabbit polyclonal antibody) secondary antibody was purchased from Santa Cruz Biotechnology (Santa Cruz, CA, USA). Secondary antibodies HRP-linked goat anti-mouse and anti-rabbit were purchased from Cell signalling (Beverly, MA, USA). Mouse monoclonal anti-IR antibody (β-subunit) was purchased from Merck Millipore (Billerica, MA, USA). Secondary antibodies Alexa Fluor 488 goat anti-rabbit and 555 goat anti-mouse were purchased from Invitrogen (Carlsbad, CA, USA). The chemiluminescent Western blot detection kit (SuperSignal West Femto Chemiluminescent Substrate) was from Thermo Scientific (Rockford, IL, USA).

Animals

Male Wistar rats (three-month-old) weighing 280-350 g (Department of Pharmacology, University of Zagreb School of Medicine) were used in the experiment. The rats were kept 2-3 per cage in a room with a 12 h light/12 h dark cycle (lights on 7 a.m. - 7 p.m.), and the room temperature and humidity set in the range of 21-23°C and 40-70%, respectively. All animals were kept on standardized food pellets and water *ad libitum*.

Drug treatments

Rats were given general anesthesia (thiopental 50 mg/kg; 5 mg/kg diazepam), followed by a single icv injection of STZ (1.5 mg/kg, dissolved in vehicle: 0.05 M citrate buffer, pH 4.5, split in two equal dose given bilaterally in a volume of 2 μl/ventricle), according to the procedure first described by Noble et al. (1967) and used in our previous experiments (Lackovic and Salkovic 1990; Grünblatt et al. 2007; Salkovic-Petrisic et al. 2013; Barilar et al. 2015; Knezovic et al. 2015). Control (CTR) animals were given an equal volume of vehicle by the same procedure. There were 8 animals per each group (CTR and STZ), all together 16 animals.

Tissue preparation

Animals were sacrificed in deep anaesthesia (thiopental 50 mg/kg; 5 mg/kg diazepam) 1 hour following the treatment. Six out of 8 animals per group were decapitated after which brains were quickly removed, hippocampus (HPC), temporal cortex (TC) and parietal cortex (PC) were dissected out and frozen in liquid nitrogen (Paxinos and Watson 2005). Since we were primarily focused to explore the regions involved in cognition, hypothalamus (HPT) has not been dissected out for Western blot analysis. Brain tissue samples for Western blot analysis were thawed and homogenized with three volumes of lysis buffer containing 10mM HEPES, 1mM EDTA, 100 mM KCl, 1% Triton X-100, pH 7,5, and a protease inhibitor cocktail (1:100) and the homogenates were centrifuged at 12000 rpm for 10 min at 4°C and the supernatant were frozen and stored at -80°C. Protein concentration was measured by Lowry protein assay. Remaining 2 animals per group were perfused with 4% paraformaldehyde, pH 7.4. Brains were removed and cryoprotected with sucrose (through series of sucrose 15% and 30%) and stored at -80°C.

Immunofluorescence

Brains were cut on cryostat (35 µm), and coronal sections were used for the free-floating immunofluorescence method. The sections were first washed with PBST (PBS buffer with 0.25% Triton X-100) and then blocked in 10% NGS in PBST. Section were then incubated overnight at 4°C with anti-GFAP antibody (1:500) and with both anti-IR and anti-GLUT2 antibodies (1:250) diluted in 1% NGS in PBST. On the second day, sections were washed with PBST and incubated with appropriate fluorescent secondary antibodies for 2h at RT. After washing in PBST, sections were mounted on slides with fluoroshield mounting medium. Slides were examined and visualized by microscope Olympus BX51 and CellSense Dimension software, and the co-expression was visualized by EMCCD microscopy camera.

Western blot analysis

Equal amounts of total protein in HPC, TC, and PC (35 µg per sample) were separated by sodium dodecyl sulphate-polyacrylamide (SDS) gel electrophoresis using 9% polyacrylamide gels and transferred to nitrocellulose membranes. The nitrocellulose membranes were blocked by incubation for 1 h at RT in 5% non-fat milk added to low-salt washing buffer (LSWB) containing 10mM Tris, 150mM NaCl, pH 7.5, and 0.5% Tween 20. Blocked blots were incubated with primary anti-GLUT2

(1:1000) and anti-IR (1:2000) antibodies overnight at 4°C. After incubation, the membranes were washed three times with LSWB and incubated for 1 h at RT with appropriate secondary antibody solution (anti-mouse and anti-rabbit IgG, 1:2000). After washing three times in LSWB signals were captured and visualized with MicroChemi video camera (DNR Bio-Imaging Systems) using chemiluminescence reagent. The membranes were washed three times with LSWB, blocked in the same way and incubated with loading control, anti-β-actin (1:2000) overnight, at 4°C. After incubation, the membranes were washed and incubated for 1 h at RT with secondary antibody solution (anti-mouse 1:2000), washed in LSWB and signals were captured and visualized with MicroChemi video camera using chemiluminescence reagent. The membranes were analysed with ImageJ software.

Since HPT has become a region of interest only after a marked neuroinflammation observed by immunofluorescence staining, and due to has not been dissected out for Western blot analysis at the time of sacrificing, GLUT2 and IR expression in HPT could have been explored only by immunofluorescence and not by Western blot.

Ethics

Animal procedures, carried out at the University of Zagreb Medical School (Zagreb, Croatia), were in compliance with current institutional, national (The Animal Protection Act, NN135/2006; NN 47/2011), and international (Directive 2010/63/EU) guidelines governing the use of experimental animals. The experiments were approved by the national regulatory body responsible for issuing ethical approval, Croatian Ministry of Agriculture and Ethical Committee, Medical School of Zagreb.

Statistics

Quantitative analysis of the GFAP positive signal was performed based on the measured area with the background subtraction done to reduce the background noise by means of CellSense Dimension imaging software. Data were expressed as mean ± SD and statistically analysed by Mann-Whitney U test ($p < 0.05$) using GraphPad Prism 5 statistical software.

RESULTS

GFAP expression in the brain

Immunoreactivity of GFAP was detected by the immunofluorescence assay and a positive signal was found in the regions of interest, cortex (TC, PC) and hippocampus (HPC), but was unexpectedly pronounced also in HPT (Fig .1). In the control group HPC was found to contain intensely stained, clearly stratified GFAP-staining, with substantially more immunoreactivity occurring in the dentate gyrus, while PC, TC, and HPT showed evenly distributed astrocytes (Fig 1A represents layer IV-V). In the STZ-icv treated animals the signal was increased in all four brain regions indicating a global neuroinflammatory response one hour after the STZ-icv treatment (Fig 1A). The quantification of the GFAP signal revealed that the increment in the STZ-icv group was significant in all four regions in comparison to the controls ($p<0.05$) (Fig. 1B). However, it was pronounced more in the PC (+109%) and the HPC (+94%) than in the TC (+70%) and the HPT (+63%) (Fig 1B). Such a regional distribution of the GFAP signal intensity may indicate the time- and concentration-dependent effect of STZ; i.e. the highest concentration close to the site of the needle breakthrough in PC and release of STZ from the needle in the vicinity of HPC, followed by spreading/diffusing of STZ diluted by CSF to more distal regions, HPT and TC (Fig 1B, C). The GFAP immunoreactivity in the cortical and the hippocampal region across and near the site of a needle injection is presented in the Supplementary material (Suppl 1).

IR and GLUT2 expression in the brain

<u>Cortex and hippocampus</u>

Positive IR immunoreactivity (red signal) was found in all brain regions of interest both in the control and the STZ-icv group (Fig 2-4). In the PC, TC and HPC, the signal was predominately on the neuronal membranes, as shown by IR – NeuN co-localization presented in the Supplementary material (Suppl 3). Mild decrement (-13%; $p<0.05$) in the IR protein expression, quantified by Western blot analysis, was found in the PC of STZ-icv group (Fig. 5), while no change in the IR level could have been quantified in the TC and HPC (Fig. 5).

Positive GLUT2 immunoreactivity (green signal) in the control and the STZ-icv group was also found in the PC, TC and HPC although less spread than the IR immunoreactivity (Fig. 2-4). Statistically significant difference in the GLUT2 protein level between the groups was found by Western blot analysis only in the HPC of the STZ-icv group which demonstrated +33% increment in comparison to the control group ($p<0.05$) (Fig. 5). This increment can be seen on the immunofluorescence photomicrographs as more intense green signal (Fig. 4). No change in the GLUT2 signal/protein expression was observed in the two cortical regions (Fig. 2-5).

Merging of the photomicrographs which detected two different immunofluorescent signals (red/IR and green/GLUT2) in the same tissue sections demonstrated co-localization of IR and GLUT2 in the particular cells of the PC, TC and HPC, seen as the yellow/orange merged signal (Fig. 2-4).

Hypothalamus

At the level of the hypothalamus, IR (red signal) and GLUT2 (green signal) immunoreactivity was found only in the ependymal lining cells of the 3rd ventricle (Fig. 6). The control group demonstrated only the IR immunoreactivity in these cells with no visible specific GLUT2 signal (Fig. 6A). In the STZ-icv group, the IR immunoreactivity in the ependymal cells was clearly reduced both in intensity and spread while the appearance of a strong signal of the GLUT2 immunoreactivity was detected in this hypothalamic area (Fig. 6A). Double immunofluorescence revealed co-expression of the GLUT2 and IR signal in the long ependymal cells, as observed by confocal microscope (Fig. 6B).

DISCUSSION

We have used the STZ-icv treated rats as a non-transgenic sAD model (Hoyer 1998; Lannert and Hoyer 1998) to explore the onset of alterations in IR and GLUT2 levels as the markers of IRBS and the cerebral glucose hypometabolism. Both are proposed to be possible etiopathogenic factors of sAD (Chen and Zhong 2013; De Felice et al. 2014; Chen et al. 2014a; de la Monte and Tong 2014). In the brain, STZ

toxicity has been associated with the neuroinflammation, reported so far to be present ≥1 week after STZ-icv administration (Salkovic-Petrisic and Hoyer 2007). Both, the GLUT2 alteration and the neuroinflammation have been detected in our experiments but the latter one appears to be more spread 1 hour after a single 1.5 mg/kg STZ-icv dose.

Neuroinflammation is a prominent and early feature of AD, which involves the activation of glial cells represented by a highly heterogeneous population of mostly microglia and astrocytes (Ransohoff, 2016). It is estimated that the astrocytes represent 30-50% of human neural cells (Lent et al, 2012) and are the most abundant type of glial cells in the brain (Steardo et al., 2015). While the role of microglia in the neuroinflammatory response to AD has been extensively explored (Heppner et al, 2015), recent data indicate that the astrocyte-mediated inflammatory processes also contribute to the neurodegeneration in AD or may even be one of the major hallmarks of this disease (Garwood et al., 2016; Verkhratsky et al., 2010). Astrocytosis was proved to be an early phenomenon in AD progression in patients with MCI and AD subjected to multitracer PET analysis (Carter et al., 2012). Astrocytosis is typically characterised by the increased expression of the astrocyte marker GFAP (Garwood et al., 2016). Human studies showed that the astrocyte hypertrophic response, characterized by the GFAP expression increases early in relation to the development of the AD neuropathology (Simpson et al., 2010). In our experiments, the STZ-icv treatment induced the extensive expression of neuroinflammation as early as 1 hour after the injection, visualized by both, the increased density and the intensity of GFAP-positive signal, especially in the parietal cortex and hippocampus, but also in the temporal cortex and the hypothalamic region. Neuroinflammation is often found in parallel with the oxidative stress, but some data also show that these two appears to be the separate events, which work in concert to modulate the development of the AD-like pathology, as shown in the transgenic mice AD model (Yao et al. 2004). In the neuroinflammatory process, astrocytes and neurons can produce/release inflammatory mediators, including reactive oxygen and nitrogen species (Agostinho et al. 2010). Additionally, oxidative stress which is implicated in the AD pathogenesis (Gsell et al. 1996; Agostinho et al. 2010), can trigger the overexpression of inducible nitric oxide synthase leading to an increased NO production (Agostinho et al. 2010). In line with that, the experiments of

Rajasekar et al. (2014) showed dose-dependent cytotoxicity of STZ in the rat astrocytoma cell line during the 24-hour incubation time, and the induction of NO release, as well as the dose- dependent generation of reactive oxidative species, the increased formation of malondialdehyde and the glutathione deficit. STZ-induced release of NO in the rat pancreatic β cells was seen already 2 hours after the treatment (Wada and Yagihashi 2004). NO was found to be liberated in β cells only when STZ had been metabolized inside the cell (Kröncke et al. 1995). The pharmacokinetics of STZ have been explored so far in rats after the parenteral administration, showing that 30% of the compound is eliminated within the first hour in the form of the degrading products and partly as the unchanged molecule (Lee et al. 1993), while in cell culture its biological half-life was shown to be approximately 19 minutes (Jensen et al. 1977). Some of its cleavage/degradation products, which chemical structure has not been clearly defined yet, were shown to have some biologic, although not diabetic, activity (Lee et al. 1993), and a capability of crossing cell membranes (Goud et al. 2015). There are no data on the STZ pharmacokinetics following its icv administration. However, the occurrence of the direct STZ effects and/or the effects of some of its cleavage/degradation products with similar characteristics to those found after the parenteral STZ administration cannot be excluded in such a short period as 1 hour after the STZ-icv injection.

Previous research suggested that the damage caused by the administration of STZ into the lateral ventricles is restricted to the brain areas near to the site of injection (Terwel et al. 1995; Shoham et al. 2003). In our experiment, the neuroinflammation induced in the vicinity of the site where STZ was released (hippocampus) was indeed highly pronounced compared to the one found after the citrate buffer injection (Suppl 1). However, our results also showed that after 1 hour, the neuroinflammation was expressed not only in the vicinity of the STZ injection and downstream the hypothalamic areas close to the cerebrospinal fluid (CSF) exposure, but also in the temporal cortex which falls in neither of the categories. The possibility that a single STZ dose injected into the lateral ventricles is capable of inducing metabolic and cytoarchitectonic responses in such a distant location as temporal cortex through a direct damage in that region, has been argued by Grieb (2016).

A possible interpretation of these findings could be that the extent and the dynamics of brain damage and the neuro/histopathological changes induced by the STZ-icv administration might depend on the amount of STZ injected as a single or cumulative dose. Kraska and coworkers (2012) followed up the progression of cerebral lesions and neuroinflammation induced in rats by the icv administration of 1 and 3 mg/kg of STZ respectively for the period of one week and up to three months after the treatment. They showed that high STZ-icv dose induced severe and acute neurodegenerative lesions restricted to the site of injection associated with the severe neuroinflammation, while the changes were less severe but more widespread and progressive at a low dose. These findings are in line with other toxic effects of STZ reported to be induced in a dose- (Rajasekar et al. 2014) and time-dependent manner (Santos et al. 2012), both found to affect the dynamics of cognitive deficits in a 9-month follow-up of STZ-icv rat model (Knezovic et al. 2015). In this respect, it is difficult to interpret neuroinflammation as well as the changes in the IR/GLUT2 expression found 1 hour after a single icv injection of 1.5 mg/kg STZ dose, in comparison with the literature data where either higher STZ-icv dose (3 mg/kg) was used to generate a model and/or the effects were observed after a period of weeks or months (as reviewed by Salkovic-Petrisic and Hoyer, 2007).

The neuroinflammation is either expressed (with or without of the possible differences in the intensity and/or distribution), or there are no signs of neuroinflammation. Contrary to that, the expression of cerebral IR/GLUT2 might additionally be susceptible to fluctuations in the metabolic status in the brain caused by STZ-icv and consequently be increased, decreased or unchanged. Our results provide the insight into the earliest changes in the expression of IR and GLUT2 in the rat brain following the STZ-icv injection. The expression of these two proteins show pronounced regional specificity. The changes are present in areas close to the site of STZ release from a needle (hippocampus /GLUT2) and downstream the CSF flow (the ependymal lining cells of the 3rd ventricle/GLUT2, IR), with either mild (IR) or no change (GLUT2) in the cortical regions. However, the observed changes were of the opposite direction, seen as increased GLUT2, and decreased IR expression.

Although the changes of the cerebral GLUT2 protein expression found 1 hour after the STZ-icv treatment appear to be opposite to the STZ-induced decrement in

GLUT2 expression in pancreatic β cells (Wang and Gleichmann 1995; Wang and Gleichmann 1998; Gai et al. 2004), it does not necessarily indicate that the mechanism of the STZ action is different after its peripheral and central administration. One speculative explanation could be that as early as 1 hour post-treatment, the neuroinflammation induced by STZ-icv treatment generates a state with the increased metabolic need which cell is trying to compensate by increasing the influx of glucose, and this may be accomplished by the increased membrane expression of GLUT2 (Kalsbeek et al. 2016). The interplay of the neuroinflammation and the oxidative stress as two separate, yet closely connected events, might have an important role here. Susceptibility to oxidative stress in the brain is regionally specific with some regions being more sensitive than the others, hippocampus in particular (Austin et al. 2015). This might provide a possible explanation why the changes in GLUT2/IR expression were not found in all investigated regions in spite of the expression of the neuroinflammation. The cell/GLUT2 responsiveness and the adjustability to the metabolic needs might be possible in this early acute phase, and at this low STZ-icv dose, but is probably lost in the course of time. This is in line with the findings in pancreatic β cells, where the STZ-induced decrement in the GLUT2 protein expression was time- and dose-dependent and first noticed 1 day after the third STZ injection (Wang and Gleichmann 1995; Wang and Gleichmann 1998; Gai et al. 2004). This hypothesis is supported by our preliminary research of GLUT2 protein and mRNA expression in the brain of the rat STZ-icv model induced by two STZ-icv injections (2x 1.5 mg/kg) and measured 1 month after the treatment (Suppl 2). These supplementary results demonstrate that the 2xfold higher STZ-icv dose and much longer post-treatment period than here are associated with the decreased expression of GLUT2 protein in the parietal and temporal cortex and the decreased GLUT2 mRNA expression in the parietal cortex. Decreased GLUT2 mRNA expression found in our supplementary experiments is in line with the similar STZ effect in the pancreatic β cells (Wang and Gleichmann 1998). Therefore, GLUT2 in the brain also appears to be the target of STZ administered into the lateral ventricles, thus one may speculate that, similarly to what happens at the periphery, the appearance of this effect in the brain is STZ-icv dose- and time-dependent.

GLUT2 is a bidirectional high-capacity glucose transporter which has been found throughout the rat brain mainly in the astrocytes but to a lesser extent also in the

neurons (Arluison et al. 2004a; Arluison et al. 2004b). The nerve cell bodies clearly immunostained for GLUT2 seem to be scarce, whereas the periphery of the numerous nerve cells is labelled for this transporter (Arluison et al. 2004b). The results presented here clearly show the GLUT2 signal in the some NeuN-positive neuronal cells in the parietotemporal cortex and hippocampus (Suppl 3). Additionally, our results also indicate the co-expression of GLUT2 and IR, observed in the regions investigated and particularly in the ependymal lining cells of the 3rd ventricle. Such a co-expression seems to be present in the skeletal muscles and liver (Rathinam and Pari 2016), however this is the first report of its presence in the rat brain. This finding may support the hypothesis that IR and its signalling pathway could be affected by STZ from the intracellular side, and not via the extracellular interaction, as argued by Grieb (2016). Also, it may not be excluded that from the intracellular side IR is the target of some biologically active degradation products of STZ, or STZ-induced oxidative stress markers. Therefore, changes in IR might be a consequence of its co-expression with the direct target of STZ (GLUT2) in the same cell. On the other hand, it cannot be excluded that IR expression is influenced by the alteration in the intracellular metabolic status, induced by increased GLUT2 expression as a response to neuroinflammation. The type of possible GLUT2-IR interaction needs to be further explored, since our results indicate that there might be an inverse correlation between the expression of GLUT2 and IR protein, at least in this early phase. However, in contrast to our preliminary findings (Suppl 2) of GLUT2 change in the opposite direction in the course of time (increment after 1 hour and decrement after 1 month), the expression of IR protein is uniformly decreased in both, the early and the late post-treatment periods, as corroborated by our results and a research of the other groups (Agrawal et al. 2011; Liu et al. 2013; Barilar et al. 2015). This may allow speculation that at low STZ dose, considering the GLUT2-IR co-expression, IR itself might be more sensitive to STZ-induced intracellular irreversible toxicity than GLUT2.

In line with the literature data that GLUT2 in the hypothalamus is expressed mainly in the astrocytes and the tanycytes (Leloup et al. 2016), our experiments show highly increased GLUT2-positive signal particularly in the ependymal lining cells of the 3rd ventricle. According to the elongated cell shape, these cells seem to be tanycytes, the main glial cells present specifically at this location (García et al. 2003). Modulation of the hypothalamic GLUT2 expression has been shown to alter glucose

sensitivity and physiological responses such as the nervous control of insulin or glucagon secretion and food intake (Leloup et al. 2016). Our results indicate that in the acute phase, this region is strongly affected by STZ-icv treatment in regard to neuroinflammation, and GLUT2/IR expression which might have important implications for the regulation of metabolic homeostasis. Although blood glucose levels have been generally found unaltered in STZ-icv rat model, as reviewed elsewhere (Salkovic-Petrisic and Hoyer 2007), some variations in plasma insulin level have been observed in our preliminary subacute experiments (unpublished data).

Conclusion

The administration of a single low STZ dose into the lateral ventricles of the adult rats induces wide spread neuroinflammation in the cortical, the hippocampal and the hypothalamic regions and more regional specific alterations in the GLUT2 and IR protein expression, which was observed as early as 1 hour after the treatment. The expression of both GLUT2 and IR was altered in areas close to the site of STZ release from a needle (hippocampus) and downstream the CSF flow (the ependymal lining cells of the 3rd ventricle) with mild or no changes observed in the parietotemporal cortex. Considering the first evidence of GLUT2 – IR co-expression in the rat brain presented here, it cannot be excluded that IR and its signalling pathway could be affected by STZ (and/or some biologically active degradation products of STZ, or STZ-induced oxidative stress markers) from the intracellular side, and not via a direct extracellular interaction. Alterations of GLUT2 and IR, as well as their co-expression in the ependymal lining cells of the 3rd ventricle, should be further explored having in mind that modulation of hypothalamic GLUT2 expression affects the regulation of metabolic homeostasis at the periphery. Cerebral GLUT2 seems to be the target molecule of STZ following its icv administration, however further research is needed to clarify whether the early GLUT2 alterations might be also induced in a response to the neuroinflammation-induced metabolic needs.

The findings of such early changes in GLUT2/IR expression and the development of neuroinflammation using the model considered to be a valuable model for sAD, might contribute to elucidate the sAD etiopathogenesis. Recent clinical study has revealed that the brain inflammation is likely to occur already at the preclinical stage of AD in MCI patients, and can be detected *in vivo* in the CSF as the increased level of

lymphocytes and pro-inflammatory cytokines IL6 and IL17 (Blum-Degen et al. 1995; Monson et al. 2014). Such an early appearance of brain inflammation in patients with preclinical AD might correspond with the neuroinflammation found here in the early phase of the STZ-icv rat model when AD-like pathological hallmarks, the early neurofibrillary changes, and the Aβ1-42 accumulation, have not appeared yet (Knezovic et al. 2015). GLUT2 expression in the brain has been poorly explored in sAD patients; post-mortem analysis showed increased GLUT2 level in the frontal cortex which disappeared after being normalized by GFAP level (Liu et al. 2008), and decreased GLUT2 mRNA in the cholinergic basal forebrain galanin-sensitive neurons (Counts et al. 2009). Although these clinical data seem to be inconclusive, they indicate that the alterations in GLUT2 in the brain might play a role in sAD pathophysiology and should be further explored, particularly regarding the possible co-expression with IR and the evidence of IRBS in sAD patients (Talbot et al. 2012).

Acknowledgements. Supported by University of Zagreb (funds awarded to M. Salkovic-Petrisic, 2015-2016), AMAC-UK (funds awarded to U. Smailovic, 2013) and the Edda Neele Stiftung (funds awarded to M. Salkovic-Petrisic). Z. Mikloska, PhD is thanked for English editing.

REFERENCES:

Agostinho P, Cunha RA, Oliveira C (2010) Neuroinflammation, oxidative stress and the pathogenesis of Alzheimer's disease. Curr Pharm Des 16:2766–78.

Agrawal R, Tyagi E, Shukla R, Nath C (2011) Insulin receptor signaling in rat hippocampus: A study in STZ (ICV) induced memory deficit model. Eur Neuropsychopharmacol 21:261–273. doi: 10.1016/j.euroneuro.2010.11.009

Agrawal R, Tyagi E, Shukla R, Nath C (2009) A study of brain insulin receptors, AChE activity and oxidative stress in rat model of ICV STZ induced dementia. Neuropharmacology 56:779–87.

Amiri S, Haj-Mirzaiain A, Momeny M, et al (2016) Streptozotocin induced oxidative stress, innate immune system responses and behavioral abnormalities in male mice. Neuroscience. doi: 10.1016/j.neuroscience.2016.11.003

Arluison M, Quignon M, Nguyen P, et al (2004a) Distribution and anatomical localization of the glucose transporter 2 (GLUT2) in the adult rat brain--an

immunohistochemical study. J Chem Neuroanat 28:117–36. doi: 10.1016/j.jchemneu.2004.05.009

Arluison M, Quignon M, Thorens B, et al (2004b) Immunocytochemical localization of the glucose transporter 2 (GLUT2) in the adult rat brain. II. Electron microscopic study. J Chem Neuroanat 28:137–46. doi: 10.1016/j.jchemneu.2004.06.002

Austin SA, Santhanam AVR, d'Uscio L V, Katusic ZS (2015) Regional Heterogeneity of Cerebral Microvessels and Brain Susceptibility to Oxidative Stress. PLoS One 10:e0144062. doi: 10.1371/journal.pone.0144062

Barilar JO, Knezovic A, Grünblatt E, et al (2015) Nine-month follow-up of the insulin receptor signalling cascade in the brain of streptozotocin rat model of sporadic Alzheimer's disease. J Neural Transm 122:565–76. doi: 10.1007/s00702-014-1323-y

Biasibetti R, Almeida Dos Santos JP, Rodrigues L, et al (2017) Hippocampal changes in STZ-model of Alzheimer's disease are dependent on sex. Behav Brain Res 316:205–214. doi: 10.1016/j.bbr.2016.08.057

Blázquez E, Velázquez E, Hurtado-Carneiro V, Ruiz-Albusac JM (2014) Insulin in the brain: its pathophysiological implications for States related with central insulin resistance, type 2 diabetes and Alzheimer's disease. Front Endocrinol (Lausanne) 5:161. doi: 10.3389/fendo.2014.00161

Blokland A, Jolles J (1993) Spatial learning deficit and reduced hippocampal ChAT activity in rats after an ICV injection of streptozotocin. Pharmacol Biochem Behav 44:491–4.

Blondel O, Portha B (1989) Early appearance of in vivo insulin resistance in adult streptozotocin-injected rats. Diabète & métabolisme 15:382–7.

Blum-Degen D, Müller T, Kuhn W, et al (1995) Interleukin-1 beta and interleukin-6 are elevated in the cerebrospinal fluid of Alzheimer's and de novo Parkinson's disease patients. Neurosci Lett 202:17–20.

Brant AM, Jess TJ, Milligan G, et al (1993) Immunological analysis of glucose transporters expressed in different regions of the rat brain and central nervous system. Biochem Biophys Res Commun 192:1297–302. doi: 10.1006/bbrc.1993.1557

Carter SF, Schöll M, Almkvist O, Wall A, Engler H, Långström B et al (2012) Evidence for astrocytosis in prodromal Alzheimer disease provided by 11C-deuterium-L-deprenyl: a multitracer PET paradigm combining 11C-Pittsburgh

compound Band 18F-FDG. J Nucl Med 53:37–46.

Chen Y, Deng Y, Zhang B, Gong C-X (2014a) Deregulation of brain insulin signaling in Alzheimer's disease. Neurosci Bull 30:282–94. doi: 10.1007/s12264-013-1408-x

Chen Y, Liang Z, Tian Z et al (2014b) Intracerebroventricular streptozotocin exacerbates Alzheimer-like changes of 3xTg-AD mice. Mol Neurobiol 49:547-62. doi: 10.1007/s12035-013-8539-y.

Chen Y, Liang Z, Blanchard J, et al (2013) A non-transgenic mouse model (icv-STZ mouse) of Alzheimer's disease: similarities to and differences from the transgenic model (3xTg-AD mouse). Mol Neurobiol 47:711–25. doi: 10.1007/s12035-012-8375-5

Chen Z, Zhong C (2013) Decoding Alzheimer's disease from perturbed cerebral glucose metabolism: Implications for diagnostic and therapeutic strategies. Prog Neurobiol 108:21–43. doi: 10.1016/j.pneurobio.2013.06.004

Correia SC, Santos RX, Santos MS, et al (2013) Mitochondrial abnormalities in a streptozotocin-induced rat model of sporadic Alzheimer's disease. Curr Alzheimer Res 10:406–19.

Counts SE, He B, Che S, et al (2009) Galanin fiber hyperinnervation preserves neuroprotective gene expression in cholinergic basal forebrain neurons in Alzheimer's disease. J Alzheimers Dis 18:885–96. doi: 10.3233/JAD-2009-1196

Cunnane S, Nugent S, Roy M, et al (2011) Brain fuel metabolism, aging, and Alzheimer's disease. Nutrition 27:3–20. doi: 10.1016/j.nut.2010.07.021

De Felice FG, Lourenco M V, Ferreira ST (2014) How does brain insulin resistance develop in Alzheimer's disease? Alzheimers Dement 10:S26-32. doi: 10.1016/j.jalz.2013.12.004

de la Monte SM, Tong M (2014) Brain metabolic dysfunction at the core of Alzheimer's disease. Biochem Pharmacol 88:548–59. doi: 10.1016/j.bcp.2013.12.012

Deng Y, Li B, Liu Y, et al (2009) Dysregulation of insulin signaling, glucose transporters, O-GlcNAcylation, and phosphorylation of tau and neurofilaments in the brain: Implication for Alzheimer's disease. Am J Pathol 175:2089–98. doi: 10.2353/ajpath.2009.090157

Dias C, Barbosa RM, Laranjinha J, Ledo A (2014) Evaluation of Mitochondrial Function in the CNS of Rodent Models of Alzheimer's Disease - High Resolution

Respirometry Applied to Acute Hippocampal Slices. Free Radic Biol Med 75 Suppl 1:S37. doi: 10.1016/j.freeradbiomed.2014.10.780

Duelli R, Schröck H, Kuschinsky W, Hoyer S (1994) Intracerebroventricular injection of streptozotocin induces discrete local changes in cerebral glucose utilization in rats. Int J Dev Neurosci 12:737–43.

Frölich L, Blum-Degen D, Bernstein HG, et al (1998) Brain insulin and insulin receptors in aging and sporadic Alzheimer's disease. J Neural Transm 105:423–38. doi: 10.1007/s007020050068

Gai W, Schott-Ohly P, Schulte im Walde S, Gleichmann H (2004) Differential target molecules for toxicity induced by streptozotocin and alloxan in pancreatic islets of mice in vitro. Exp Clin Endocrinol Diabetes 112:29–37. doi: 10.1055/s-2004-815724

García M de los A, Millán C, Balmaceda-Aguilera C, et al (2003) Hypothalamic ependymal-glial cells express the glucose transporter GLUT2, a protein involved in glucose sensing. J Neurochem 86:709–724. doi: 10.1046/j.1471-4159.2003.01892.x

Garwood CJ, Ratcliffe LE, Simpson JE, Heath PR, Ince PG, Wharton SB (2016) Review: Astrocytes in Alzheimer's disease and other age-associated dementias; a supporting player with a central role. Neuropathol Appl Neurobiol, doi: 10.1111/nan.12338. [Epub ahead of print]

Giorgino F, Chen JH, Smith RJ (1992) Changes in tyrosine phosphorylation of insulin receptors and a 170,000 molecular weight nonreceptor protein in vivo in skeletal muscle of streptozotocin-induced diabetic rats: effects of insulin and glucose. Endocrinology 130:1433–44. doi: 10.1210/endo.130.3.1531627

Goud BJ, Dwarakanath.V, Swamy BKC (2015) Streptozotocin – A Diabetogenic Agent in Animal Models. Int J Pharm Pharm Res 3:253–269.

Grieb P (2016) Intracerebroventricular Streptozotocin Injections as a Model of Alzheimer's Disease: in Search of a Relevant Mechanism. Mol Neurobiol 53:1741–52. doi: 10.1007/s12035-015-9132-3

Grünblatt E, Salkovic-Petrisic M, Osmanovic J, et al (2007) Brain insulin system dysfunction in streptozotocin intracerebroventricularly treated rats generates hyperphosphorylated tau protein. J Neurochem 101:757–770. doi: 10.1111/j.1471-4159.2006.04368.x

Gsell W, Strein I, Riederer P (1996) The neurochemistry of Alzheimer type, vascular

type and mixed type dementias compared. J Neural Transm Suppl 47:73–101.
Heppner R, Ransohoff R, Becher B (2015) Immune attack: the role of inflammation in Alzheimer disease. Nat Rev Neurosci 16:358-72.
Hoyer S (1998) Is sporadic Alzheimer disease the brain type of non-insulin dependent diabetes mellitus? A challenging hypothesis. J Neural Transm 105:415–22. doi: 10.1007/s007020050067
Hoyer S, Lannert H (2007) Long-term abnormalities in brain glucose/energy metabolism after inhibition of the neuronal insulin receptor: implication of tau-protein. J Neural Transm Suppl 195–202.
Hoyer S, Müller D, Plaschke K (1994) Desensitization of brain insulin receptor. Effect on glucose/energy and related metabolism. J Neural Transm Suppl 44:259–68.
Jensen EM, LaPolla RJ, Kirby PE, Haworth SR (1977) In vitro studies of chemical mutagens and carcinogens. I. Stability studies in cell culture medium. J Natl Cancer Inst 59:941–4.
Kadowaki T, Kasuga M, Akanuma Y, et al (1984) Decreased autophosphorylation of the insulin receptor-kinase in streptozotocin-diabetic rats. J Biol Chem 259:14208–16.
Kalsbeek MJT, Mulder L, Yi C-X (2016) Microglia energy metabolism in metabolic disorder. Mol Cell Endocrinol. doi: 10.1016/j.mce.2016.09.028
Knezovic A, Osmanovic-Barilar J, Curlin M, et al (2015) Staging of cognitive deficits and neuropathological and ultrastructural changes in streptozotocin-induced rat model of Alzheimer's disease. J Neural Transm 122:577–92. doi: 10.1007/s00702-015-1394-4
Konrad RJ, Mikolaenko I, Tolar JF, et al (2001) The potential mechanism of the diabetogenic action of streptozotocin: inhibition of pancreatic beta-cell O-GlcNAc-selective N-acetyl-beta-D-glucosaminidase. Biochem J 356:31–41.
Kraska A, Santin MD, Dorieux O, et al (2012) In vivo cross-sectional characterization of cerebral alterations induced by intracerebroventricular administration of streptozotocin. PLoS One 7:e46196. doi: 10.1371/journal.pone.0046196
Kröncke KD, Fehsel K, Sommer A, et al (1995) Nitric oxide generation during cellular metabolization of the diabetogenic N-methyl-N-nitroso-urea streptozotozin contributes to islet cell DNA damage. Biol Chem Hoppe Seyler 376:179–85.
Lacković Z, Salković M (1990) Streptozotocin and alloxan produce alterations in rat brain monoamines independently of pancreatic beta cells destruction. Life Sci

46:49–54.

Lannert H, Hoyer S (1998) Intracerebroventricular administration of streptozotocin causes long-term diminutions in learning and memory abilities and in cerebral energy metabolism in adult rats. Behav Neurosci 112:1199–208.

Lee JY, Kim MJ, Moon CK, Chung JH (1993) Degradation products of streptozotocin do not induce hyperglycemia in rats. Biochem Pharmacol 46:2111–3.

Leloup C, Allard C, Carneiro L, et al (2016) Glucose and hypothalamic astrocytes: More than a fueling role? Neuroscience 323:110–20. doi: 10.1016/j.neuroscience.2015.06.007

Lent R, Azevedo FA, Andrade-Moraes CH, Pinto AV (2012) How many neurons do you have? Some dogmas of quantitative neuroscience under revision. Eur J Neurosci 35:1–9.

Lester-Coll N, Rivera EJ, Soscia SJ, et al (2006) Intracerebral streptozotocin model of type 3 diabetes: relevance to sporadic Alzheimer's disease. J Alzheimers Dis 9:13–33.

Li D, Huang Y, Cheng B, et al (2016) Streptozotocin Induces Mild Cognitive Impairment at Appropriate Doses in Mice as Determined by Long-Term Potentiation and the Morris Water Maze. J Alzheimer's Dis 54:89–98. doi: 10.3233/JAD-150979

Liu P, Zou L, Jiao Q, et al (2013) Xanthoceraside attenuates learning and memory deficits via improving insulin signaling in STZ-induced AD rats. Neurosci Lett 543:115–20. doi: 10.1016/j.neulet.2013.02.065

Liu Y, Liu F, Iqbal K, et al (2008) Decreased glucose transporters correlate to abnormal hyperphosphorylation of tau in Alzheimer disease. FEBS Lett 582:359–64. doi: 10.1016/j.febslet.2007.12.035

Maekawa F, Toyoda Y, Torii N, et al (2000) Localization of glucokinase-like immunoreactivity in the rat lower brain stem: for possible location of brain glucose-sensing mechanisms. Endocrinology 141:375–84. doi: 10.1210/endo.141.1.7234

Mayer G, Nitsch R, Hoyer S (1990) Effects of changes in peripheral and cerebral glucose metabolism on locomotor activity, learning and memory in adult male rats. Brain Res 532:95–100.

Monson NL, Ireland SJ, Ligocki AJ, et al (2014) Elevated CNS inflammation in patients with preclinical Alzheimer's disease. J Cereb Blood Flow Metab 34:30–

3. doi: 10.1038/jcbfm.2013.183

Mosconi L (2005) Brain glucose metabolism in the early and specific diagnosis of Alzheimer's disease. FDG-PET studies in MCI and AD. Eur J Nucl Med Mol Imaging 32:486–510. doi: 10.1007/s00259-005-1762-7

Mosconi L, Mistur R, Switalski R, et al (2009) Declining brain glucose metabolism in normal individuals with a maternal history of Alzheimer disease. Neurology 72:513–20. doi: 10.1212/01.wnl.0000333247.51383.43

Noble EP, Wurtman RJ, Axelrod J (1967) A simple and rapid method for injecting H3-norepinephrine into the lateral ventricle of the rat brain. Life Sci 6:281–291. doi: 10.1016/0024-3205(67)90157-9

Paxinos G, Watson C (2005) The Rat Brain in Stereotaxic Coordinates, 5th edn. Elsevier Academic Press

Plaschke K, Hoyer S (1993) Action of the diabetogenic drug streptozotocin on glycolytic and glycogenolytic metabolism in adult rat brain cortex and hippocampus. Int J Dev Neurosci 11:477–83.

Plaschke K, Kopitz J, Siegelin M, et al (2010) Insulin-resistant brain state after intracerebroventricular streptozotocin injection exacerbates Alzheimer-like changes in Tg2576 AbetaPP-overexpressing mice. J Alzheimers Dis 19:691–704. doi: 10.3233/JAD-2010-1270

Prakash A, Kalra JK, Kumar A (2015) Neuroprotective effect of N-acetyl cysteine against streptozotocin-induced memory dysfunction and oxidative damage in rats. J Basic Clin Physiol Pharmacol 26:13–23. doi: 10.1515/jbcpp-2013-0150

Prickaerts J, Fahrig T, Blokland A (1999) Cognitive performance and biochemical markers in septum, hippocampus and striatum of rats after an i.c.v. injection of streptozotocin: a correlation analysis. Behav Brain Res 102:73–88. doi: 10.1016/S0166-4328(98)00158-2

Rajasekar N, Dwivedi S, Nath C, et al (2014) Protection of streptozotocin induced insulin receptor dysfunction, neuroinflammation and amyloidogenesis in astrocytes by insulin. Neuropharmacology 86:337–52. doi: 10.1016/j.neuropharm.2014.08.013

Ransohoff RM (2016) How neuroinflammation contributes to neurodegeneration. Science 353:777-83.

Rathinam A, Pari L (2016) Myrtenal ameliorates hyperglycemia by enhancing GLUT2 through Akt in the skeletal muscle and liver of diabetic rats. Chem Biol Interact

256:161–6. doi: 10.1016/j.cbi.2016.07.009

Reiman EM, Caselli RJ, Yun LS, et al (1996) Preclinical evidence of Alzheimer's disease in persons homozygous for the epsilon 4 allele for apolipoprotein E. N Engl J Med 334:752–8. doi: 10.1056/NEJM199603213341202

Salkovic-Petrisic M, Hoyer S (2007) Central insulin resistance as a trigger for sporadic Alzheimer-like pathology: an experimental approach. J Neural Transm Suppl 217–33.

Salkovic-Petrisic M, Knezovic A, Hoyer S, Riederer P (2013) What have we learned from the streptozotocin-induced animal model of sporadic Alzheimer's disease, about the therapeutic strategies in Alzheimer's research. J Neural Transm 120:233–52. doi: 10.1007/s00702-012-0877-9

Salkovic-Petrisic M, Osmanovic-Barilar J, Brückner MK, et al (2011) Cerebral amyloid angiopathy in streptozotocin rat model of sporadic Alzheimer's disease: a long-term follow up study. J Neural Transm 118:765–72. doi: 10.1007/s00702-011-0651-4

Salkovic-Petrisic M, Tribl F, Schmidt M, et al (2006) Alzheimer-like changes in protein kinase B and glycogen synthase kinase-3 in rat frontal cortex and hippocampus after damage to the insulin signalling pathway. J Neurochem 96:1005–15. doi: 10.1111/j.1471-4159.2005.03637.x

Santos TO, Mazucanti CHY, Xavier GF, Torrão AS (2012) Early and late neurodegeneration and memory disruption after intracerebroventricular streptozotocin. Physiol Behav 107:401–13. doi: 10.1016/j.physbeh.2012.06.019

Saxena G, Singh SP, Agrawal R, Nath C (2008) Effect of donepezil and tacrine on oxidative stress in intracerebral streptozotocin-induced model of dementia in mice. Eur J Pharmacol 581:283–289. doi: 10.1016/j.ejphar.2007.12.009

Sharma M, Gupta YK (2001) Intracerebroventricular injection of streptozotocin in rats produces both oxidative stress in the brain and cognitive impairment. Life Sci 68:1021–9.

Shoham S, Bejar C, Kovalev E, Weinstock M (2003) Intracerebroventricular injection of streptozotocin causes neurotoxicity to myelin that contributes to spatial memory deficits in rats. Exp Neurol 184:1043–1052. doi: 10.1016/j.expneurol.2003.08.015

Simpson JE, Ince PG, Lace G, Forster G, Shaw PJ, Matthews F, Savva G, Brayne C, Wharton SB (2010) Astrocyte phenotype in relation to Alzheimer-type pathology

in the ageing brain. Neurobiol Aging 3:578-90.

Stanley M, Macauley SL, Holtzman DM (2016) Changes in insulin and insulin signaling in Alzheimer's disease: cause or consequence? J Exp Med 213:1375–85. doi: 10.1084/jem.20160493

Steardo LJr, Bronzuoli MR, Iacomino A, Esposito G, Steardo L, Scuderi C (2015) Does neuroinflammation turn on the flame in Alzheimer's disease? Focus on astrocytes. Front Neurosci 9:259. doi: 10.3389/fnins.2015.00259. eCollection 2015.

Steen E, Terry BM, Rivera EJ, et al (2005) Impaired insulin and insulin-like growth factor expression and signaling mechanisms in Alzheimer's disease--is this type 3 diabetes? J Alzheimers Dis 7:63–80.

Szkudelski T (2001) The mechanism of alloxan and streptozotocin action in B cells of the rat pancreas. Physiol Res 50:537–46.

Talbot K (2014) Brain insulin resistance in Alzheimer's disease and its potential treatment with GLP-1 analogs. Neurodegener Dis Manag 4:31–40. doi: 10.2217/nmt.13.73

Talbot K, Wang H-Y, Kazi H, et al (2012) Demonstrated brain insulin resistance in Alzheimer's disease patients is associated with IGF-1 resistance, IRS-1 dysregulation, and cognitive decline. J Clin Invest 122:1316–38. doi: 10.1172/JCI59903

Terwel D, Prickaerts J, Meng F, Jolles J (1995) Brain enzyme activities after intracerebroventricular injection of streptozotocin in rats receiving acetyl-L-carnitine. Eur J Pharmacol 287:65–71.

Verkhratsky A, Olabarria M, Noristani HN, Yeh CY, Rodriguez JJ (2010) Astrocytes in Alzheimer's disease. Neurotherapeutics 7:399-412. doi: 10.1016/j.nurt.2010.05.017

Wada R, Yagihashi S (2004) Nitric oxide generation and poly(ADP ribose) polymerase activation precede beta-cell death in rats with a single high-dose injection of streptozotocin. Virchows Arch 444:375–382. doi: 10.1007/s00428-003-0967-z

Wang Z, Gleichmann H (1995) Glucose transporter 2 expression: prevention of streptozotocin-induced reduction in beta-cells with 5-thio-D-glucose. Exp Clin Endocrinol Diabetes 83–97. doi: 10.1055/s-0029-1211400

Wang Z, Gleichmann H (1998) GLUT2 in pancreatic islets: crucial target molecule in

diabetes induced with multiple low doses of streptozotocin in mice. Diabetes 47:50–6.

Yao Y, Chinnici C, Tang H, et al (2004) Brain inflammation and oxidative stress in a transgenic mouse model of Alzheimer-like brain amyloidosis. J Neuroinflammation 1:21. doi: 10.1186/1742-2094-1-21

Yarchoan M, Toledo JB, Lee EB, et al (2014) Abnormal serine phosphorylation of insulin receptor substrate 1 is associated with tau pathology in Alzheimer's disease and tauopathies. Acta Neuropathol 128:679–89. doi: 10.1007/s00401-014-1328-5

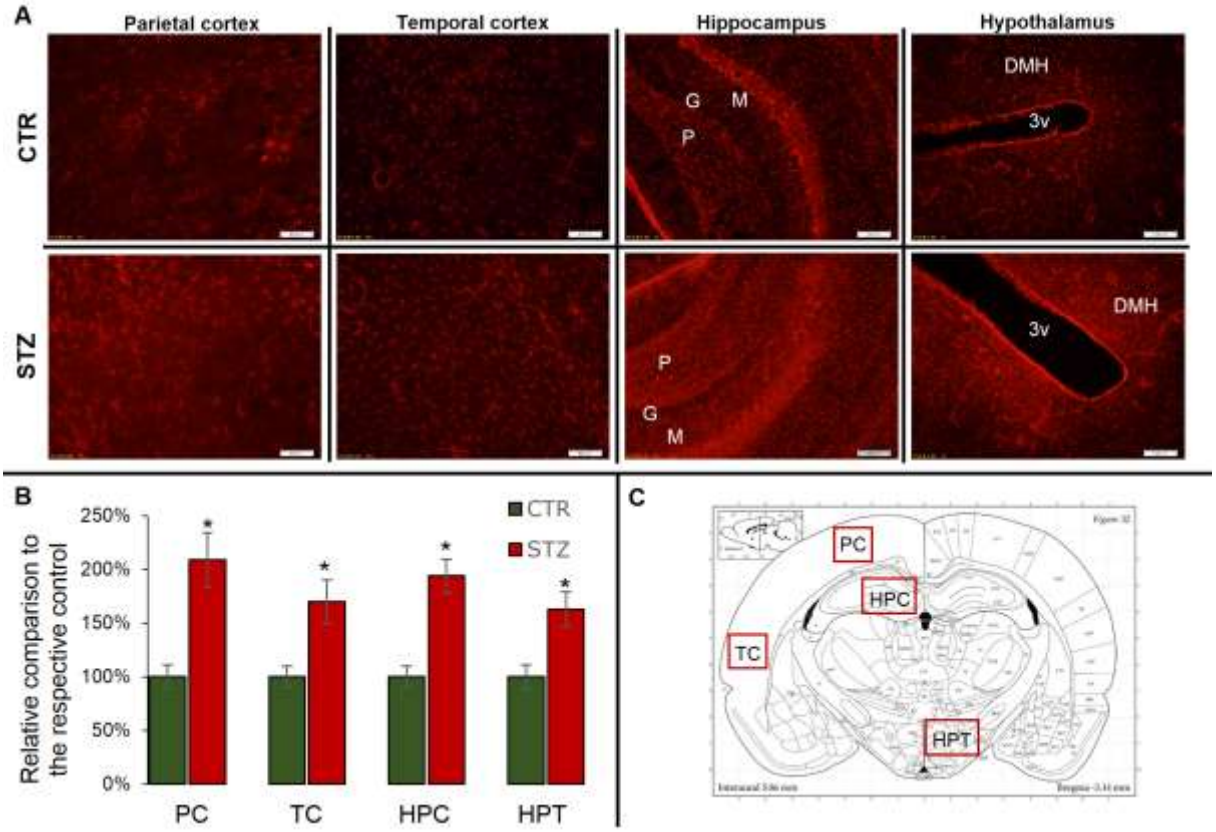

Fig 1. Immunoreactivity of the glial fibrillary acidic protein expression in the brain of streptozotocin-treated rats visualized by immunofluorescence. Animals were euthanized 1 hour after intracerebroventricular (icv) treatment with streptozotocin (STZ) (1.5 mg/kg) or vehicle (CTR). Slides with brain sections (35 μm thick slices) were subjected to immunofluorescence staining with the glucose transporter-2 (GLUT2) and the insulin receptor (IR) antibodies. Representative photomicrographs (the same exposition used for STZ and CTR slides in the same region) show the positive glial fibrillary acidic protein (GFAP) expression (red signal) detected one hour after icv injection in hippocampus (HPC), hypothalamus (HPT), parietal (PC) and temporal (TC) cortices (both in the cortical layer IV-V) (**A**). Quantitative analysis of the positive GFAP signal was performed by means of CellSense Dimension imaging software. Six sections per brain of each animal were analysed and the mean ± SEM value of the group was presented as a bar in a relative comparison to the area-matched respective control (**B**). Investigated regions are marked at the brain map, with a notification that PC and TC have not been at the same interaural and/or Bregma level (**C**). Statistical analysis was done by Mann-Whitney U test (*$p<0.05$ compared to the control). Scale bar = 200 μm (HPC and HPT); 100 μm (PC and TC). Hippocampus - Dentate gyrus: P=polymorphic layer,

G=granular layer, M=molecular layer; Hypothalamus – 3v=3rd ventricle, DMH=dorsomedial hypothalamic nucleus

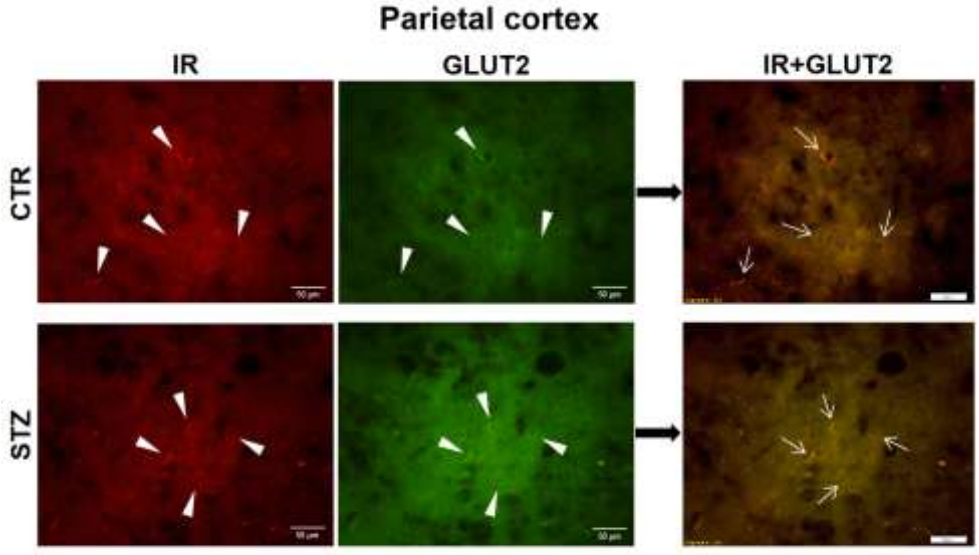

Fig 2. Immunofluorescence staining of insulin receptor and glucose transporter-2 in the parietal cortex of the streptozotocin-treated rats. Animals were euthanized 1 hour after the intracerebroventricular (icv) treatment with streptozotocin (STZ) (1.5 mg/kg) or vehicle (CTR). Slides with brain sections (35 μm thick slices) were subjected to double immunofluorescence staining with the glucose transporter-2 (GLUT2) and the insulin receptor (IR) antibodies. Representative photomicrographs show the positive GLUT2 and IR signal in the parietal cortex (layers IV-V) seen as a green and red staining, respectively, detected one hour following the treatment. Single cells with a positive signal are indicated by the white arrowheads. The signal was then merged by CellSence Dimension software, and representative cells with co-expression of IR and GLUT2 (IR+GLUT2) indicated by the white arrows. Scale bar = 50 μm.

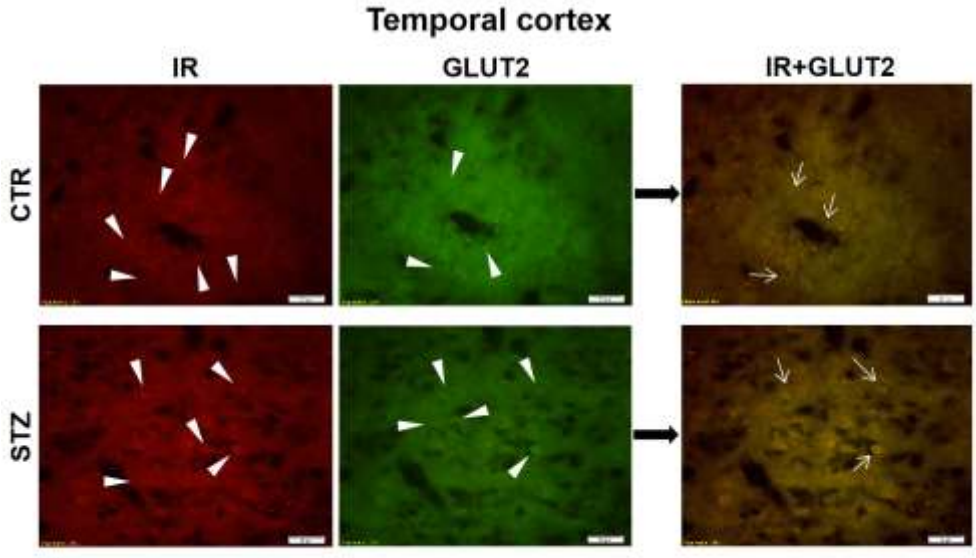

Fig 3. Immunofluorescence staining of insulin receptor and glucose transporter-2 in the temporal cortex of the streptozotocin-treated rats. Animals were euthanized 1 hour after the intracerebroventricular (icv) treatment with streptozotocin (STZ) (1.5 mg/kg) or vehicle (CTR). Slides with brain sections (35 μm thick slices) were subjected to double immunofluorescence staining with glucose transporter-2 (GLUT2) and the insulin receptor (IR) antibodies. Representative photomicrographs show the positive GLUT2 and IR signal in the temporal cortex (layers IV-V) seen as a green and red staining, respectively, detected one hour following the treatment. Single cells with a positive signal are indicated by the white arrowheads. The signal was then merged by CellSence Dimension software, and representative cells with co-expression of IR and GLUT2 (IR+GLUT2) indicated by the white arrows. Scale bar = 50 μm.

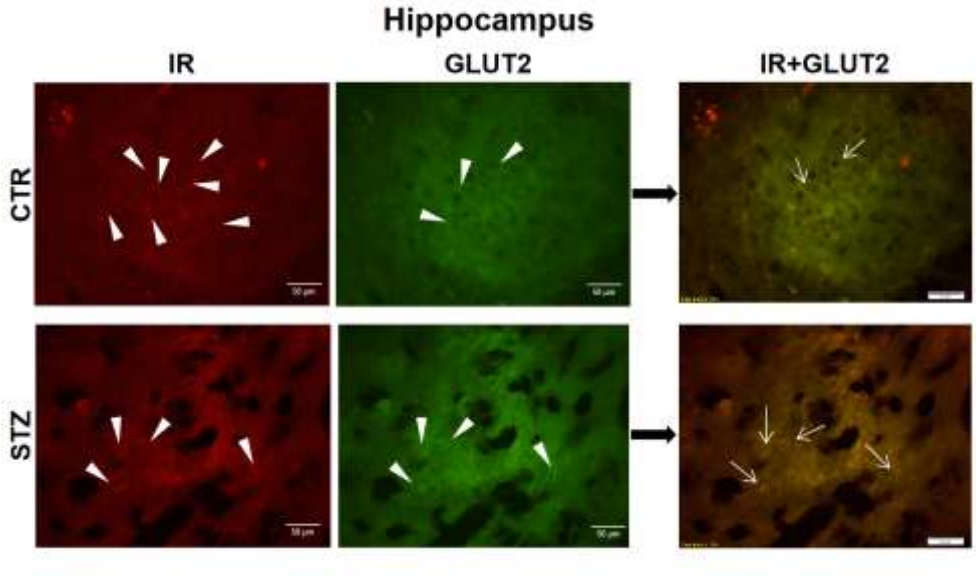

Fig 4. Immunofluorescence staining of insulin receptor and glucose transporter-2 in the hippocampus of the streptozotocin treated rats. Animals were euthanized 1 hour after the intracerebroventricular (icv) treatment with streptozotocin (STZ) (1.5 mg/kg) or vehicle (CTR). Slides with brain sections (35 μm thick slices) were subjected to double immunofluorescence staining with the glucose transporter-2 (GLUT2) and the insulin receptor (IR) antibodies. Representative photomicrographs show a positive GLUT2 and IR signal in the polymorphic layer of dentate gyrus seen as a green and red staining, respectively, detected one hour following the treatment. Single cells with a positive signal are indicated by the white arrowheads. The signal was then merged by CellSence Dimension software, and representative cells with co-expression of IR and GLUT2 (IR+GLUT2) indicated by the white arrows. Scale bar = 50 μm.

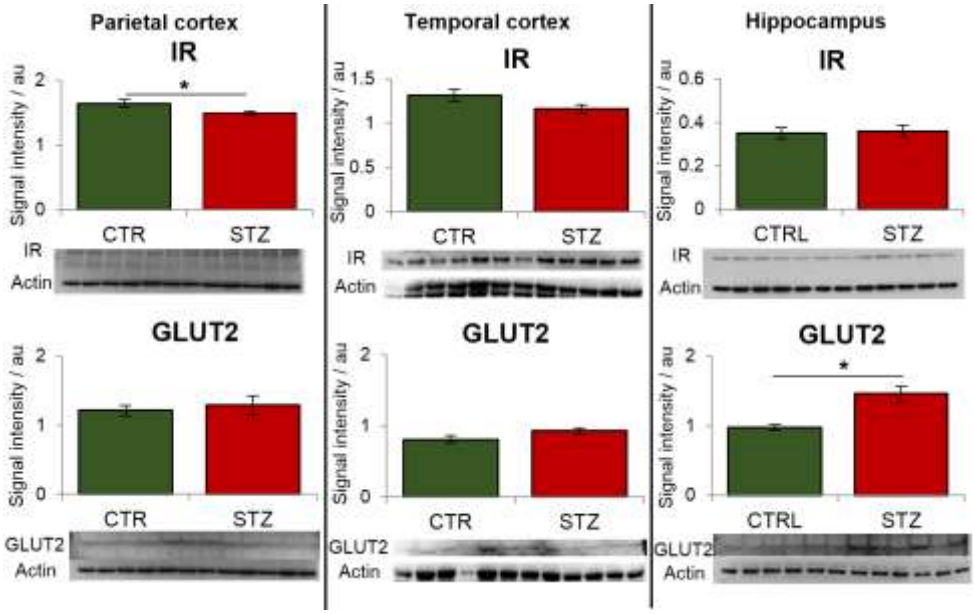

Fig 5. Glucose transporter-2 and insulin receptor protein expression in the hippocampus and the cerebral cortices (parietal and temporal) of the streptozotocin-intracerebroventricularly treated rats. Animals were euthanized 1 hour after the intracerebroventricular (icv) treatment with streptozotocin (STZ-icv) (1.5 mg/kg) or vehicle (CTR). Glucose transporter-2 (GLUT2) and insulin receptor (IR) protein expressions in the parietal (PC) and temporal (TC) cortex and the hippocampus (HPC) were measured by Western blot analysis with the representative blots being presented. Anti-β-actin was used as a loading control. Each bar (mean±SEM) represents relative ratio of signal intensity expressed by arbitrary units (au) for CTR and STZ. *p<0.05 vs CTR by Mann Whitney U test.

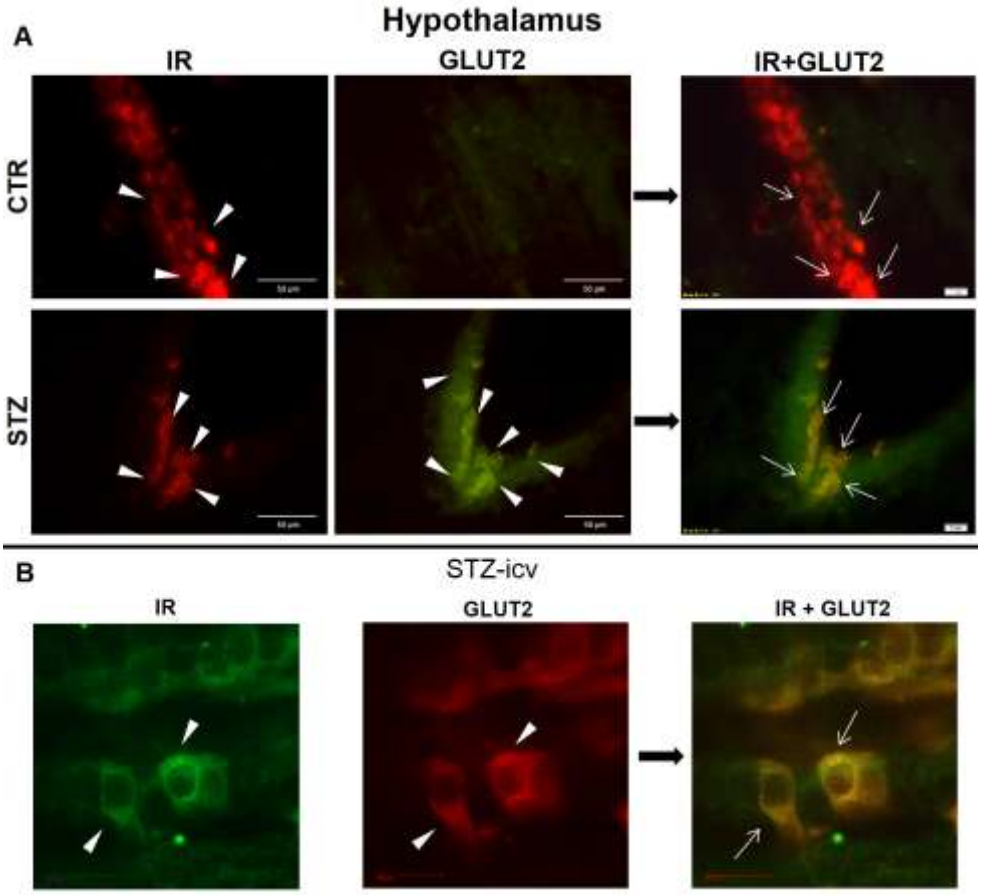

Fig 6. The effect of intracerebroventricular treatment of streptozotocin on the expression of glucose transporter-2 and insulin receptor in the rat hypothalamus. Animals were euthanized 1 hour after the intracerebroventricular (icv) treatment with streptozotocin (STZ) (1.5 mg/kg) or vehicle (CTR). Slides with brain sections (35 μm thick slices) were subjected to immunofluorescence staining with the glucose transporter-2 (GLUT2) and the insulin receptor (IR) antibodies. Representative photomicrographs of the hypothalamic region at the level of dorsomedial hypothalamic nucleus show a positive GLUT2 and IR signal in the cells of ependymal lining of the 3rd ventricle seen as a green and red staining, respectively. Single cells with a positive signal are indicated by the white arrowheads. The signal was then merged by CellSence Dimension software, and representative cells with co-expression of IR and GLUT2 (IR+GLUT2) indicated by the white arrows. (**A**). IR+GLUT2 co-expression (indicated by the white arrows) in these cells was further visualized by confocal microscope (**B**). Scale bar = 50 μm and 10 μm for confocal microscope photomicrographs.

Suppl 1. The effect of intracerebroventricular treatment of streptozotocin on the expression of glial fibrillary acidic protein in the area of needle injection. (A) The figures shows representative photomicrographs in the area of needle injection across the parietal cortex of streptozotocin (STZ) treated rats and age matched controls (CTR) one hour following the intracerebroventricular (icv) treatment, in the experiment described in the main text (Material and methods). A strong red signal of glial fibrillary acidic protein (GFAP) was found in the vicinity of a needle penetration through the parietal cortex of both groups, with intensive signal seen also in the hippocampal region (gyrus dentatus) particularly in the STZ-icv group (A) and in the ependymal lining of lateral ventricle **(B)** as well as on the cortical surface **(C)**. White arrows indicate the needle penetration site (A). HPC, hippocampus; PC , parietal cortex; v, lateral ventricle. Scale bar = 200 µm (A), 100 µm (B) and 50 µm (C).

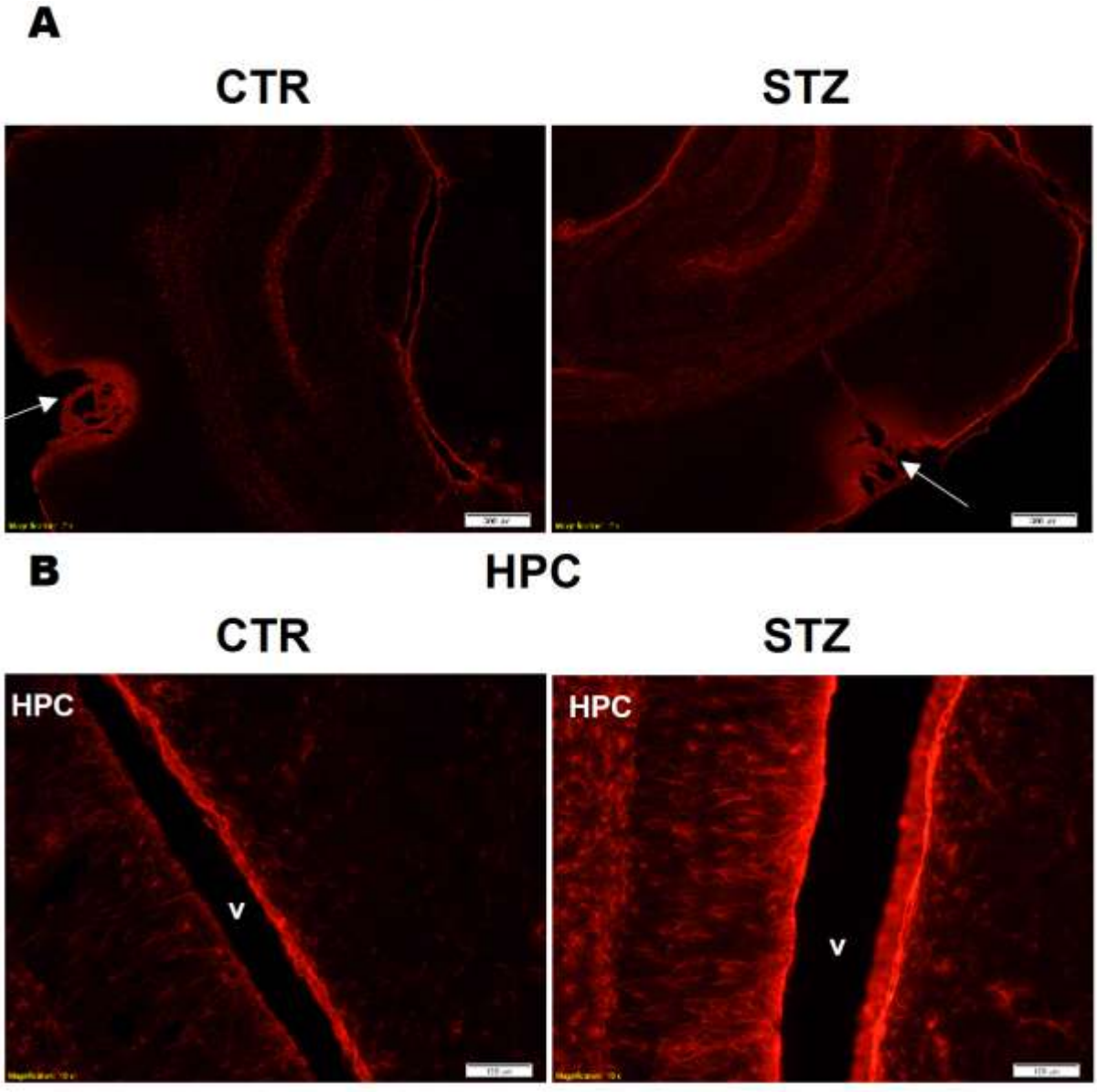

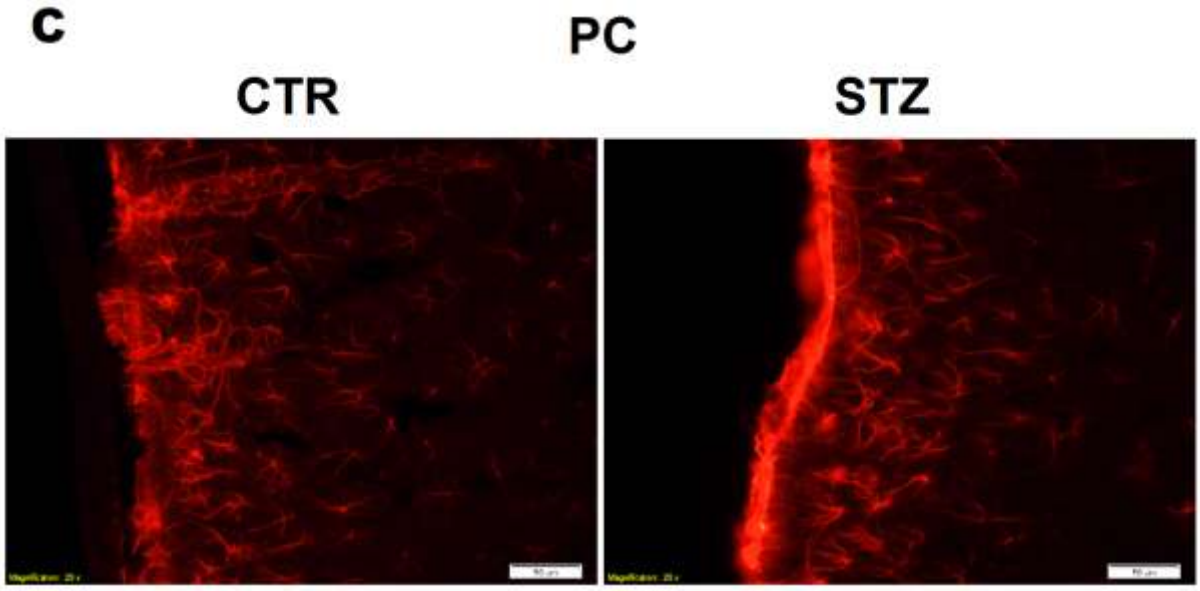
C
PC
CTR
STZ

Suppl 2. GLUT2 protein and mRNA expression in brain regions of STZ-icv treated rats measured 1 month following the icv administration of 3 mg/kg STZ dose

Animals

Male Wistar rats (three-month-old) weighing 280-350 g (Department of Pharmacology, University of Zagreb School of Medicine) were used in the separate experiment. The rats were kept 2-3 per cage in a room with a 12 h light/12 h dark cycle (lights on 07:00 – 19:00 h), and the room temperature and humidity set in the range of 21-23°C and 40-70% respectively. All animals were kept on standardized food pellets and water *ad libitum*.

Drug treatments

Intracerebroventricular (icv) treatment was performed as described in the main text (Material and methods) with streptozotocin (STZ) given in two doses, on the first and third day (each time 1.5 mg/kg, dissolved in vehicle: 0.05 M citrate buffer, pH 4.5, bilaterally 2 μl/ventricle) to rats subjected to deep anesthesia (thiopental 40 mg/kg; 4 mg/kg diazepam). The total STZ dose was 3 mg/kg. Control (CTR) animals were given an equal volume of vehicle by the same procedure on the first and third day. There were 6 animals per each group (CTR and STZ), all together 12 animals.

Tissue preparation

Animals were sacrificed in deep anesthesia (thiopental 50 mg/kg; 5 mg/kg diazepam) 1 month following the treatment. After decapitation brains were quickly removed, with hippocampus (HPC), temporal cortex (TC) and parietal cortex (PC) being dissected out and frozen in liquid nitrogen. One side of the brain was used for Western blot analysis for glucose transporter 2 (GLUT2) by a procedure described in the main text (Material and methods) and the other side was used for real-time PCR analysis.

Real-time RT-PCR - methodology

Total RNA was isolated from each area of each rat brain region following the manual of a TRIzol®Plus RNA Purification Kit (Thermo Fisher Scientific, Foster City, CA, USA), and RNA quantity was determined by OD A_{260}/A_{280}. The experiment for relative quantification of gene expression was performed on an Applied Biosystems 7500 Real-Time PCR System using *Relative Quantitation Using Comparative CT (SDS v 2.0.6 Software)* (Thermo Fisher Scientific, Foster City, CA, USA). Serial 10-fold dilutions of a representative sample were used initially to assess that the efficiency of each gene PCR was 90–110%. Cycle threshold (Ct) was obtained for each sample. A corrected Ct (ΔCt) was calculated by subtracting the Ct from the target gene Glut2 Ct for each sample. Relative differences from the control sample were then calculated by using the formula: fold change 2^ (control ΔCt -sample ΔCt) (Schmittgen and Livak, 2008). Analysis was carried out as a one-step RT-PCR, the protocol is set by Li et al. (2003) and TaqMan® RNA-to-CT™ 1-Step Kit protocol. The reaction mixture contained: 100 ng RNA, 500 nM forward primers, 500 nM reverse primers, 200 nm TaqMan® probes, TaqMan® RT-PCR Mix (2X) and TaqMan® RT Enzyme Mix (40X) (Thermo Fisher Scientific, Foster City, CA, USA). Primers and probes for cyclophilin (CYC) and glucose transporter 2 (GLUT2) (Table 1.)

Table 1. Primer and probe sequences for real-time RT-PCR		
Name	Sequence 5'-3'	GenBank
Cyc	F: CCCACCGTGTTCTTCGACAT R: TGCAAACAGCTCGAAGCAGA P: CAAGGGCTCGCCATCAGCCG	M19533
Glut2	F: GTCCAGAAAGCCCCAGATACC R: TGCCCCTTAGTCTTTTCAAGCT P: TTGCCCTGACTTCCTCTTCCAAATTTAGGTAA	NM 012879

The reaction condition was: 48°C for 15 min for RT; one cycle of 95°C for 10 min plus 40 cycles of 95°C for 15 s and 60°C for 1 min for PCR. The mRNA level of GLUT2 gene was expressed as its ratio to internal control gene– cyclophilin (CYC). Data are reported as means ±S.E.M. Fold effects of glucose transporter 2 (GLUT2) expression in STZ treated rats was compared to untreated rats and was determined after normalization with CYC expression.

Statistics

The significance between group differences (mean ± SD) was tested by Mann-Whitney U test, with significance set at $p \leq 0.05$.

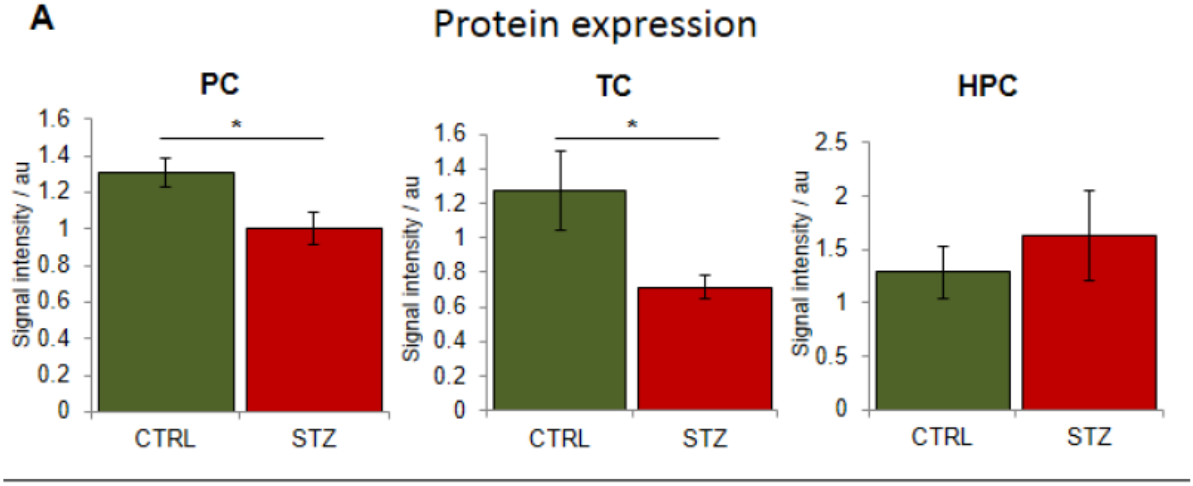

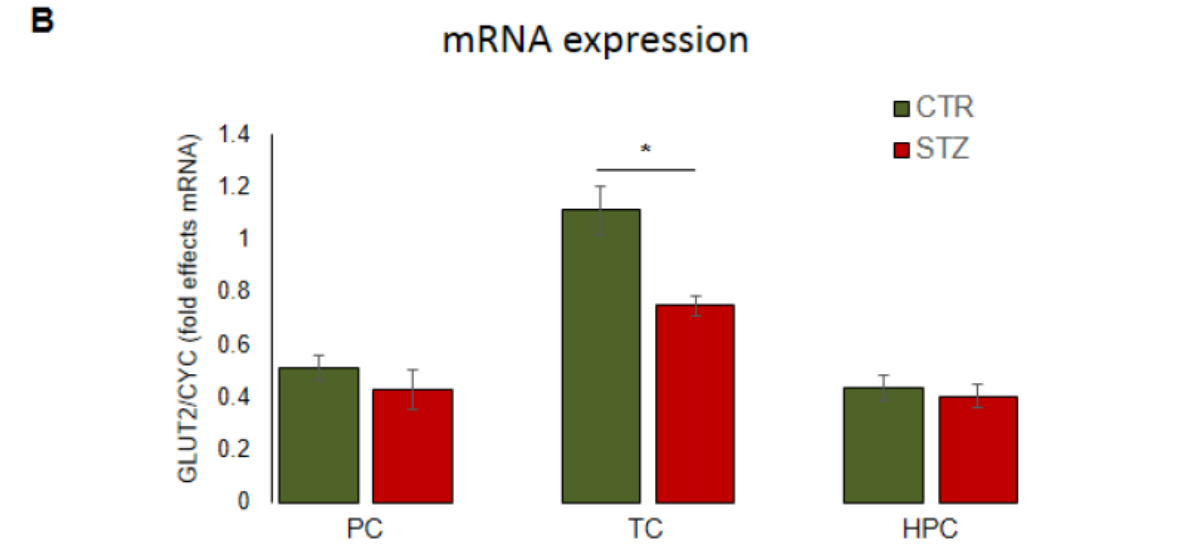

Figure 1. Protein and mRNA glucose transporter 2 expression in hippocampus and parietal and temporal cortices. Animals were euthanized 1 month after intracerebroventricular (icv) treatment with streptozotocin (STZ-icv) (1.5 mg/kg) or vehicle (CTR). Glucose transporter 2 (GLUT2) protein expression in cortices (parietal/PC and temporal/TC) and hippocampus (HPC) were measured by Western blot analysis with the representative blots being presented (**A**). β-actin was used as a loading control. Each bar (mean±SEM) represents relative ratio of signal intensity presented with arbitrary units (au) for CTR and STZ (**A**). Relative expression of GLUT2 mRNA in TC, PC, and HPC in CTR and STZ groups was measured by real-time RT-PCR. Expression of GLUT2 was normalized to expression of cyclophilin (CYC) and then fold effects were determined by comparing expression of GLUT2 in TC, PC, and HPC to expression in random TC sample. Each bar represents the mean ±S.E.M. of 4-6 experiments (and each experiment contained three samples that were also averaged) (**B**). *$p<0.05$ vs CTR by Mann-Whitney U test for both analysis.

Literature:

Li B, Xi X, Roane DS, Ryan DH, Martin RJ. Distribution of glucokinase, glucose transporter GLUT2, sulfonylurea receptor-1, glucagon-like peptide-1 receptor and neuropeptide Y messenger RNAs in rat brain by quantitative real time RT-PCR. Brain Res Mol Brain Res. 2003;113(1-2):139-42.

Schmittgen TD, Livak KJ. Analyzing real-time PCR data by the comparative C(T) method. Nat Protoc. 2008;3(6):1101-8.

Suppl 3. Insulin receptor and NeuN co-expression

Immunohistochemistry - methodology

Brains were cut on crystat (35 µm) and coronal sections were used for the free-floating immunohistochemical method. Sections were first washed with PBST (PBS buffer with 0.25% Triton X-100) and then blocked in 10% NGS in PBST. After that sections were incubated overnight at 4°C with anti-insulin receptor (IR) antibody (1:250) in 1% NGS in PBST. On the second day, sections were washed with PBST and incubated with appropriate fluorescent secondary antibody (1:400) for 2h at RT. After washing in PBST sections were incubated in darkness in preheated acidic elution buffer (50°C, pH=2) containing 1% sodium dodecyl sulfate for 30 min without shaking and then blocked again (Matak et al., 2014). After the overnight incubation with another primary antibody anti-NeuN (neuronal marker; 1:2000; purchased from Merck Millipore (Billerica, MA, USA)) at 4°C sections were incubated with appropriate fluorescent secondary antibody (1:600) for 2h at RT. Sections were mounted on slides with fluoroshield mounting medium. Slides were examined and visualized by microscope Olympus BX51 and pictures were merged with CellSense Dimension software.

Literature:

Matak I, Rossetto O, Lackovic Z (2014) Botulinum toxin type A selectivity for certain types of pain is associated with capsaicin-sensitive neurons. Pain 155:1516-26.

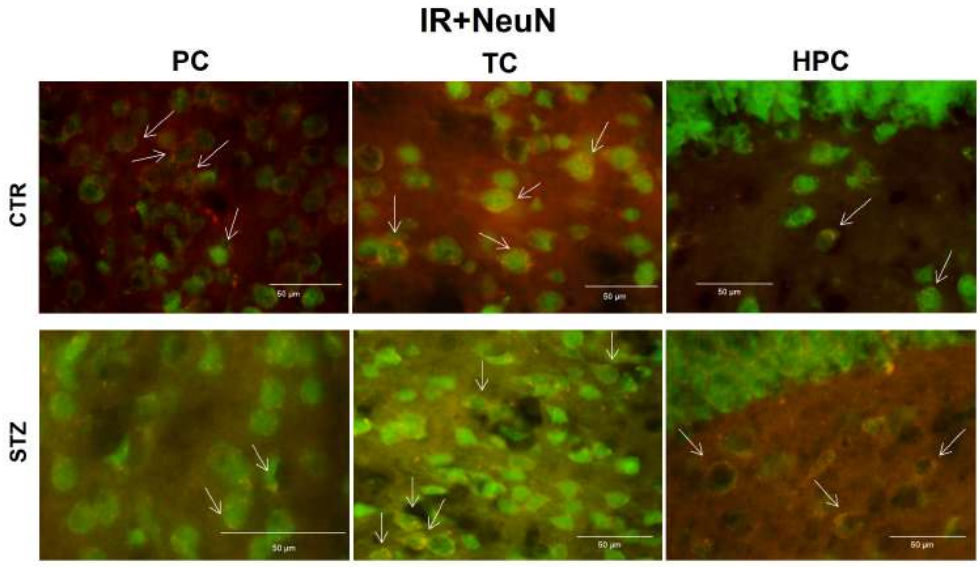

Figure 1. Immunofluorescence staining of insulin receptor and neuronal NeuN marker in parietal and temporal cortices and hippocampus of streptozotocin-intracerebroventricularly treated rats. The figure shows representative photomicrographs of the parietal cortex (PC), temporal cortex (TC) and hippocampus (HPC) from the streptozotocin (STZ) treated rats and age matched controls (CTR) that were sacrificed one hour following the intracerebroventricular treatment. The red signal represents insulin receptor (IR) and green signal neuronal marker NeuN expression. The signal was then merged by cellSence Dimension which showed the co-expression (yellow signal) of IR and NeuN (IR+NeuN) in some of the neurons (white arrows indicate representative signal). Scale bar = 50 µm.